www.oncotarget.com Oncotarget, 2018, Vol. 9, (No. 74), pp: 33896-33911

Research Paper

Inhibition of store-operated channels by carboxyamidotriazole sensitizes ovarian carcinoma cells to anti-Bclx$_L$ strategies through Mcl-1 down-regulation

Marie-Laure Bonnefond[1,2,*], Romane Florent[1,2,*], Sophie Lenoir[3], Bernard Lambert[1,2,4], Edwige Abeilard[1,2], Florence Giffard[1,2], Marie-Hélène Louis[1,2], Nicolas Elie[1,5], Mélanie Briand[1,2,6], Denis Vivien[3], Laurent Poulain[1,2], Pascal Gauduchon[1,2] and Monique N'Diaye[1,2]

[1]Normandie University, UNICAEN, INSERM U1086 ANTICIPE, Interdisciplinary Research Unit for Cancer Prevention and Treatment, BioTICLA Axis, Biology and Innovative Therapeutics for Ovarian Cancers, Caen, France

[2]UNICANCER, François Baclesse Cancer Center, BioTICLA Laboratory, Caen, France

[3]Normandie University, UNICAEN, INSERM UMR-S 1237, Physiopathologie et Imagerie des Troubles Neurologiques (PhIND), tPA and Neurovascular Disorders Team, Caen, France

[4]Délégation Régionale de Normandie, CNRS, Caen, France

[5]Normandie University, UNICAEN, Centre de Microscopie Appliqué à la Biologie, CMabio3, Structure Fédérative 4206 ICORE, Caen, France

[6]Centre de Ressources Biologiques, OvaRessources, François Baclesse Cancer Center, Caen, France

[*]These authors have contributed equally to this work

Correspondence to: *Monique N'Diaye,* ***email:*** *monique.ndiaye@unicaen.fr*

Keywords: *ovarian cancer; Store-operated calcium channels; mTORC1; MCL-1; ABT-737*

Received: *October 27, 2017* ***Accepted:*** *August 04, 2018* ***Published:*** *September 21, 2018*

ABSTRACT

The anti-apoptotic proteins Bcl-x$_L$ and Mcl-1 have been identified to play a pivotal role in apoptosis resistance in ovarian cancer and constitute key targets for innovative therapeutic strategies. Although BH3-mimetics (i.e. ABT-737) potently inhibit Bcl-x$_L$ activity, targeting Mcl-1 remains a hurdle to the success of these strategies. Calcium signaling is profoundly remodeled during carcinogenesis and was reported to activate the signaling pathway controlling Mcl-1 expression. In this context, we investigated the effect of carboxyamidotriazole (CAI), a calcium channel inhibitor used in clinical trials, on Mcl-1 expression. CAI had an anti-proliferative effect on ovarian carcinoma cell lines and strongly down-regulated Mcl-1 expression. It inhibited store-operated calcium entry (SOCE) and Mcl-1 translation through mTORC1 deactivation. Moreover, it sensitized ovarian carcinoma cells to anti-Bcl-x$_L$ strategies as their combination elicited massive apoptosis. Its effect on mTORC1 and Mcl-1 was mimicked by the potent SOCE inhibitor, YM58483, which also triggered apoptosis when combined with ABT-737. As a whole, this study suggests that CAI sensitizes to anti-Bcl-x$_L$ strategies *via* its action on Mcl-1 translation and that modulation of SOCE could extend the therapeutic arsenal for treatment of ovarian carcinoma.

INTRODUCTION

Despite its low incidence, epithelial ovarian carcinoma (EOC) is the fifth-leading cause of cancer-related deaths in women. It was estimated that in 2017, there would be more than 22240 new cases of ovarian cancers and 14080 deaths in the United States [1]. The standard treatment consists of wide-margin surgical resection and a platinum-based chemotherapy in combination with paclitaxel [2]. Despite a good response

to first-line chemotherapy, 80% of patients relapse during the first 18 months due to chemoresistance. Escape from apoptosis is one of the major hallmarks of cancer cells and is frequently due to alteration of the ratio of [anti- versus pro-apoptotic] members of the Bcl-2 family, which leads to an increase in apoptotic threshold during oncogenic stress [3]. This altered ratio could be a therapeutic opportunity and it is widely accepted that targeting anti-apoptotic members is a relevant strategy to induce apoptosis in many types of cancer [4]. Our group previously showed that the anti-apoptotic proteins Mcl-1 and Bcl-x_L were able to cooperate to allow ovarian carcinoma cells to overcome apoptosis, as their concomitant inhibition was sufficient to induce cell death [5–7]. These proteins are now considered as relevant targets for the treatment of chemoresistant ovarian cancers, and the identification of adequate strategies for their efficient inhibition constitutes an exciting challenge.

The crucial role of Bcl-x_L in cancers has led to the development of many tools to counteract its anti-apoptotic effect such as BH3-mimetics. These molecules, which mimic the BH3 domain of pro-apoptotic proteins, can hinder the function of anti-apoptotic proteins by binding their hydrophobic groove. Among these molecules, ABT-263 (Navitoclax), the orally administrable derivative of ABT-737, is currently undergoing phase I and II clinical trials in different locations including ovarian cancer (NCT02591095). However, ABT-737 does not target Mcl-1 and overexpression of this protein constitutes a hurdle to ABT-737-induced apoptosis [6].

Several strategies have been tested to inhibit Mcl-1 expression or activity. Among these, the benefit of PI3K/Akt/mTOR inhibitors to control Mcl-1 expression was investigated. Targeting this survival pathway is a key objective for gynecological cancer therapy as it is overactivated in almost half of high-grade serous ovarian tumors. Moreover, mTORC1 is known to control Mcl-1 translation through 4E-BP1 phosphorylation [8–13]. In this context, the combination of PI3K/Akt/mTOR inhibitor with ABT-737 induced apoptosis in various cancer types including ovarian cancers *in vitro* and *in vivo* PDX models [14–17].

Among the different possibilities to impede PI3K/Akt/mTOR activation, the role of calcium has been under study for several years and is particularly attractive. Calcium is the most important second messenger in the cell and it regulates fundamental physiological events such as gene expression, survival and cell death. Its impact on cell fate depends on the fine regulation of the amplitude and/or frequency of its signal [18–21]. As cancer cells require intense metabolism for their growth and motility, carcinogenesis often occurs with the modulation of calcium homeostasis (via modulation of calcium channels and pumps) for supplying cancer cells and activating pro-survival pathways [21–23]. Several studies have shown that mTORC1 is a target for calcium [24–31]. Recently, we showed that calcium chelation by BAPTA-AM and calmodulin inhibition by W7 led to a decrease in Mcl-1 *via* down-regulation of the mTORC1/4E-BP1 pathway and sensitized ovarian cancer cells to anti-Bcl-x_L strategies [13].

Modulating calcium signaling is now viewed as an emerging anti-tumoral strategy but only a few calcium inhibitors have been included in clinical trials to date [20, 21]. One of them, carboxyamidotriazole (CAI), was shown to have anti-tumoral and anti-angiogenic properties *in vitro* and *in vivo* through its ability to inhibit calcium channels such as Store-Operated Calcium Channels (SOC)[32–40]. CAI and its pro-drug salt form (carboxyamidotriazole orotate - CTO) have reached several clinical trials in various solid cancers including ovarian carcinoma, cervical cancer, renal cell carcinoma, melanoma or glioblastoma [41–48]. Reported results showed that CAI used as a single agent or in combination with paclitaxel or temozolomide has a well-tolerated toxicity profile with low grade side-effects such as fatigue, nausea or reversible peripheral neuropathy. CAI exhibited mild anticancer properties in some clinical trials, however it was described to stabilize 31% of patients with relapsed ovarian cancer for more than 6 months and its combination with Temozolomide displayed effective antitumor activity in glioblastoma [45, 48]. As we previously showed that Mcl-1 is a target for calcium signaling, we investigated whether CAI could modulate the expression of Mcl-1, with a special attention to the molecular mechanism involved and whether it could sensitize platinum-refractory ovarian cancer cells to anti-Bcl-x_L strategies.

RESULTS

CAI inhibits Mcl-1 expression and has an anti-proliferative effect on ovarian carcinoma cells

The expression of the Bcl-2 family anti-apoptotic members was analyzed in IGROV1-R10, OVCAR3 and SKOV3 cell lines treated with increasing concentrations of CAI from 24h to 72h. Whereas no variation in Mcl-1 expression was noticed in the three cell lines after 24h of treatment, a drastic decrease was observed from 48h of treatment in IGROV1-10 and from 72h of treatment in OVCAR3 and SKOV3 cells (Figure 1A). This decrease appeared from 2.5 μM of CAI and was accentuated for 5 μM. Regarding the other anti-apoptotic members, Bcl-x_L expression was not down-regulated by CAI and was instead slightly induced after 72h of treatment in OVCAR3 and SKOV3, but not IGROV1-R10 cells (Figure 1A). Bcl-2 was not expressed in IGROV1-R10 cells as previously described [13] and was not significantly modulated upon CAI treatment for OVCAR3 and SKOV3 (Figure 1A).

The study of the impact of CAI on these cell lines proliferation showed that from a concentration of 2.5 μM, CAI exerted an anti-proliferative effect which was

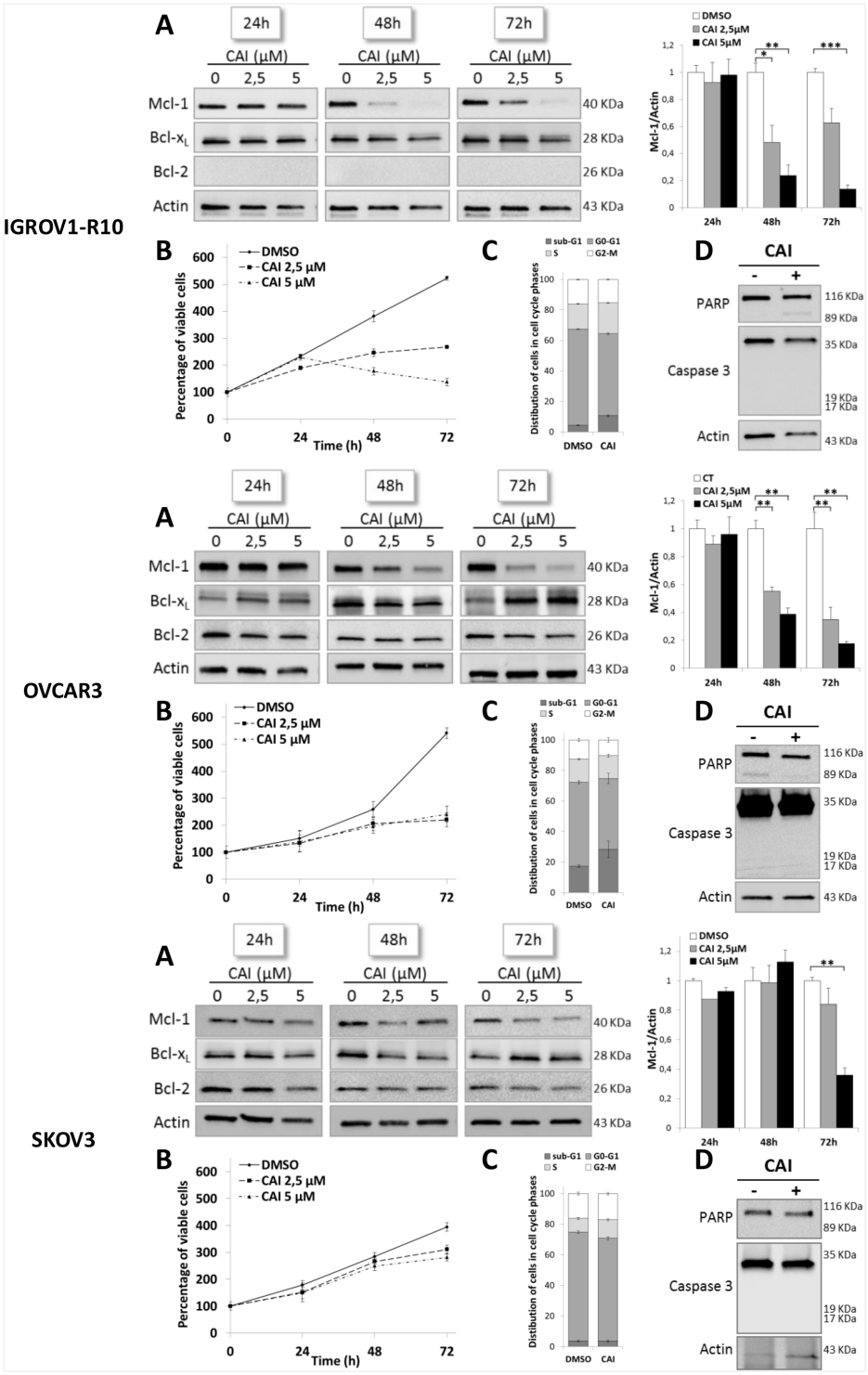

Figure 1: CAI inhibits Mcl-1 protein expression and has an anti-proliferative effect on three ovarian cell lines. (A) Expressions of Mcl-1, Bcl-x_L and Bcl-2 were assessed by western blot in IGROV1-R10, OVCAR3 and SKOV3. Cells were treated by increasing concentrations of CAI for 24h, 48h and 72h. Mcl-1 protein expression upon CAI treatment in the three cell lines tested was quantified with Image J software. Data are expressed as mean ± SEM of three independent experiments. Statistical differences were analyzed with a Student t-test: $^{*}p< 0.05$, $^{**}p< 0.01$, $^{***}p< 0.001$ (n=3). **(B)** Number of viable cells was assessed by blue trypan exclusion. Curves show the percentage of viable cells normalized to the number of viable cells at the beginning of treatment (100%). Results are expressed as mean ± SEM of three independent experiments (n=3). **(C)** Histograms represent the distribution of cells in cell cycle phases (sub-G1, G0-G1, S and G2-M) induced by 5 µM CAI for 48h (IGROV1-R10 cells) and 72h (for OVCAR3 and SKOV3 cells) and studied by flow cytometry. Results are expressed as mean ± SEM of three independent experiments. **(D)** The effect of 5µM CAI on PARP and caspase 3 cleavages was assessed by western blot for 24h, 48h and 72h in IGROV1-R10, OVCAR3 and SKOV3 cell lines.

observed after 48h in IGROV1-R10 cells and after 72h in OVCAR3 and SKOV3 cells (Figure 1B). Nevertheless, it was not accompanied by a significant blockade in cell cycle phases. In conditions leading to Mcl-1 inhibition (5μM / 48h for IGROV1-R10, 5μM / 72h for OVCAR3 and SKOV3), CAI did not induce apoptosis, a finding confirmed by the absence of sub-G1 peak and PARP and caspase 3 cleavages (Figure 1C and 1D). Therefore, CAI-induced Mcl-1 inhibition is not a consequence of cell death or cleavage by caspase 3 [49]. Moreover, the absence of cell death could be ascribed to Bcl-x_L maintenance in response to CAI.

Store-mediated Ca^{2+} entry is inhibited in ovarian carcinoma cell lines by CAI treatment

As CAI is known to inhibit various calcium channels, we attempted to identify the nature of the channels it targets in ovarian carcinoma models [32–37]. For this purpose, store-operated calcium entry (SOCE) was evaluated by using "Ca^{2+} re-addition" methodology [50]. SOCE is an ubiquitous extracellular Ca^{2+} entry pathway. Upon calcium RE depletion by IP3 receptor (IP3R) opening, the Ca^{2+} sensor molecules STIM-1 (Stromal Interaction Molecule-1) aggregate on the RE surface and physically interact with ORAI 1 proteins (Calcium release-activated calcium channel protein 1) located on the plasma membrane. This leads to the formation of a store-operated channel (SOC) that allows calcium influx from the extracellular medium [51].

Cells were thus placed in a Ca^{2+}-free HBBSS medium with 2 μM thapsigargin, an inhibitor of sarcoplasmic-endoplasmic reticulum Ca^{2+}-ATPase (SERCA), in order to deplete calcium from the endoplasmic reticulum. Upon this treatment, IGROV1-R10, OVCAR3 and SKOV3 cells exhibited a rapid rise in $[Ca^{2+}]_i$ reflecting calcium release from RE *via* the IP3 receptor [52]. Subsequent addition of 2 mM $CaCl_2$ to the extracellular medium triggered a sustained increase in $[Ca^{2+}]_i$ from baseline (x4.23 in IGROV1-R10, x2.66 in OVCAR3 and x7.28 in SKOV3), which is consistent with a characteristic SOCE-mediated Ca^{2+} influx from the extracellular solution (Figure 2A and 2B). The experiment reiterated with cells pretreated for 1 hour with 5 μM CAI showed that whereas CAI did not inhibit calcium release from IP3R, it potently inhibited SOCE in the three cell lines (Figure 2A and 2B). Altogether, this strongly suggests that CAI inhibits store-operated calcium channels in ovarian carcinoma cells.

CAI-induced Mcl-1 inhibition is not transcriptional or post-translational but is correlated with inhibition of mTORC1 pathway

To decipher the mechanisms underlying Mcl-1 down-regulation in response to CAI, Mcl-1 mRNA expression was quantified by using RT-qPCR. Treatment of cells with 5 μM CAI for 24h and 48h (IGROV1-R10) or 48h and 72h (OVCAR3 and SKOV3) did not inhibit Mcl-1 expression at mRNA level (Figure 3A), suggesting that CAI induced Mcl-1 down-regulation through transcription-independent mechanisms.

To investigate whether the Mcl-1 decrease upon CAI treatment was a consequence of proteasomal degradation, we incubated ovarian carcinoma cells with CAI for 48h (IGROV1-R10) or 72h (OVCAR3 and SKOV3) but supplemented the medium with bortezomib, a proteasome inhibitor, for the last 24 hours before analysis. As depicted in Figure 3B, bortezomib alone inhibited Mcl-1 degradation, which led to a strong up-regulation of Mcl-1 protein expression in the three cell lines tested. However, when CAI was added, bortezomib did not prevent the loss of Mcl-1 protein triggered by CAI. This suggests that CAI inhibits Mcl-1 protein through mechanisms upstream of proteasomal degradation, perhaps via translational events.

Therefore, we assessed the impact of CAI on the Akt/mTOR pathway, which is known to control Mcl-1 translation. Treatment with CAI dose-dependently inhibited mTORC1 activation in the three cell lines, as reflected by a decrease in P-mTORC1(Ser2448), P-4E-BP1 and P-p70S6K (Figure 3C). In agreement with previous reports, P-mTORC1(Ser2448) inhibition led to a feedback loop that triggered a transient up-regulation of P-Akt(Thr308) and P-Akt(Ser473) [53, 54], an effect that was observed in OVCAR3 and SKOV3 cell lines. Regarding IGROV1-R10, although P-Akt(Thr308) was also up-regulated, CAI treatment dose-dependently inhibited P-Akt(Ser473), suggesting that it inhibits both mTORC2 and P-Akt(Ser473) [53]. Thus, despite context-dependent effects on Akt activation, these results suggest that CAI down-regulates Mcl-1 translation through mTORC1 inhibition in ovarian carcinoma cells.

We then investigated the molecular link between SOCE inhibition and the decrease in mTORC1 phosphorylation. For this purpose, we evaluated the involvement of CamKII, a calcium/calmodulin-stimulated serine/threonine protein kinase acting as one of the major calcium sensors in the cell. CamKII was described to modulate several cellular processes such as carcinogenesis by controlling cancer cell survival including mTOR activation [55, 56]. Phosphorylated CamKII (Thr286) was expressed in the three cell lines at basal level, but CAI did not inhibit its activation (Supplementary Data 1), suggesting that CamKII is not involved in Mcl-1 inhibition induced by SOCE down-regulation.

Moreover, mTORC1 is known to be negatively controlled by phosphorylated AMP-activated protein kinase (p-AMPK) [57]. As CAI inhibited mTORC1, we then tested whether it was able to induce AMPK activation in our models. However, as illustrated in Supplementary Data 1, CAI did not trigger AMPK activation in the three cell lines, suggesting that AMPK was not involved in

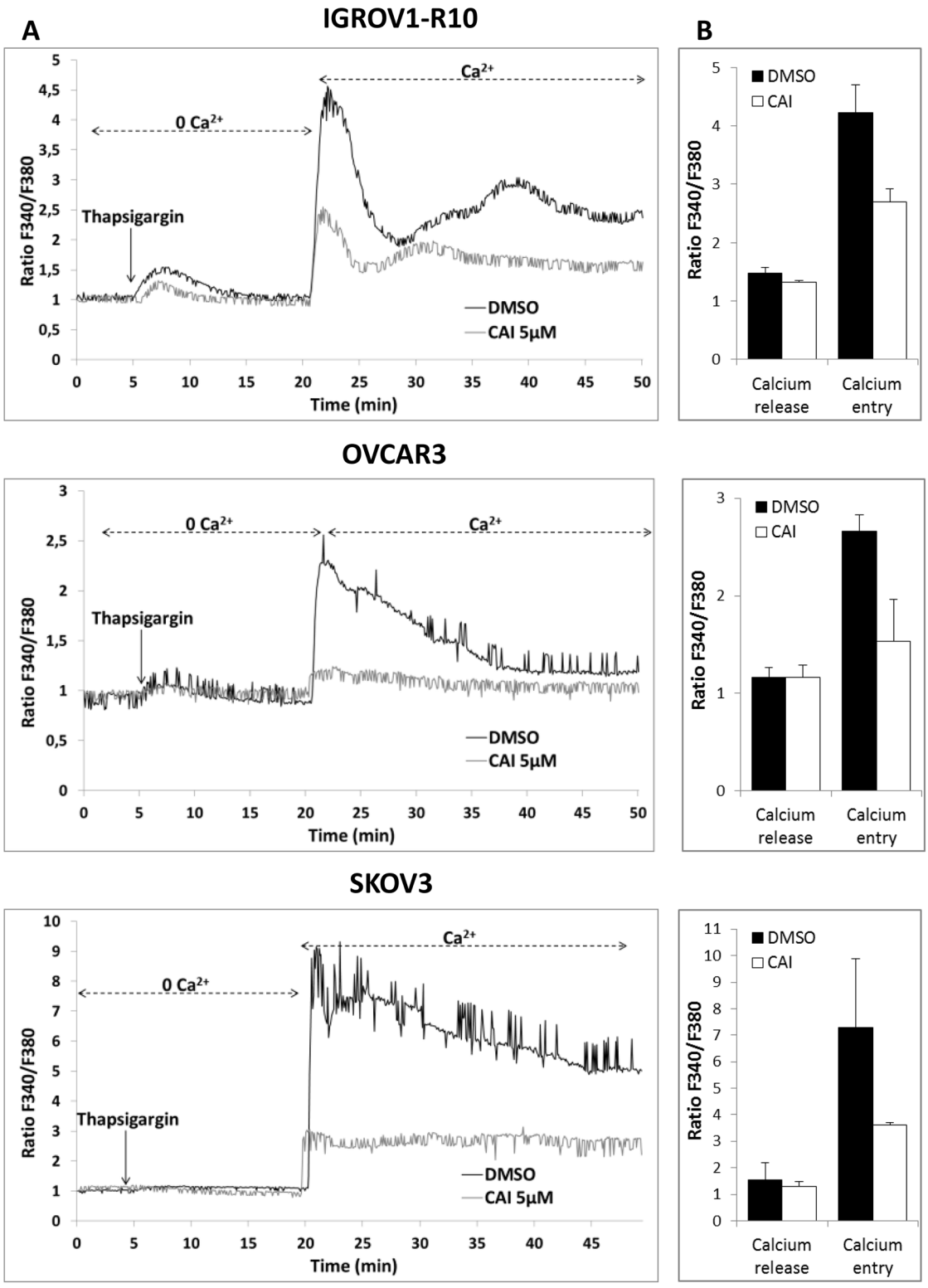

Figure 2: CAI does not block IP3R calcium release but inhibits SOCE. (A) Effect of CAI on IP3R and SOC. Microspectrofluorimetry using Fura-2AM probe was performed in the three carcinoma cell lines IGROV1-R10, OVCAR3 and SKOV3 cells. During exposure to 0Ca^{2+}, depletion of the intracellular stores was triggered by the addition of 2 µM thapsigargin to the bathing medium. Subsequent replenishment of 2 mM Ca^{2+} to the medium elicited a rise in $[Ca^{2+}]_i$ due to Ca^{2+} influx through open SOC. Black tracings depict the representative changes in $[Ca^{2+}]_i$ recorded from DMSO-treated cells and grey tracings depict the representative changes in $[Ca^{2+}]_i$ recorded from cells pre-treated for 1h with 5µM CAI. **(B)** Means ± SEM of the peaks of thapsigargin-induced Ca^{2+} release and Ca^{2+} store-operated channel entry recorded from CAI pre-treated cells (black bar) or not (DMSO) (white bar) (n=3).

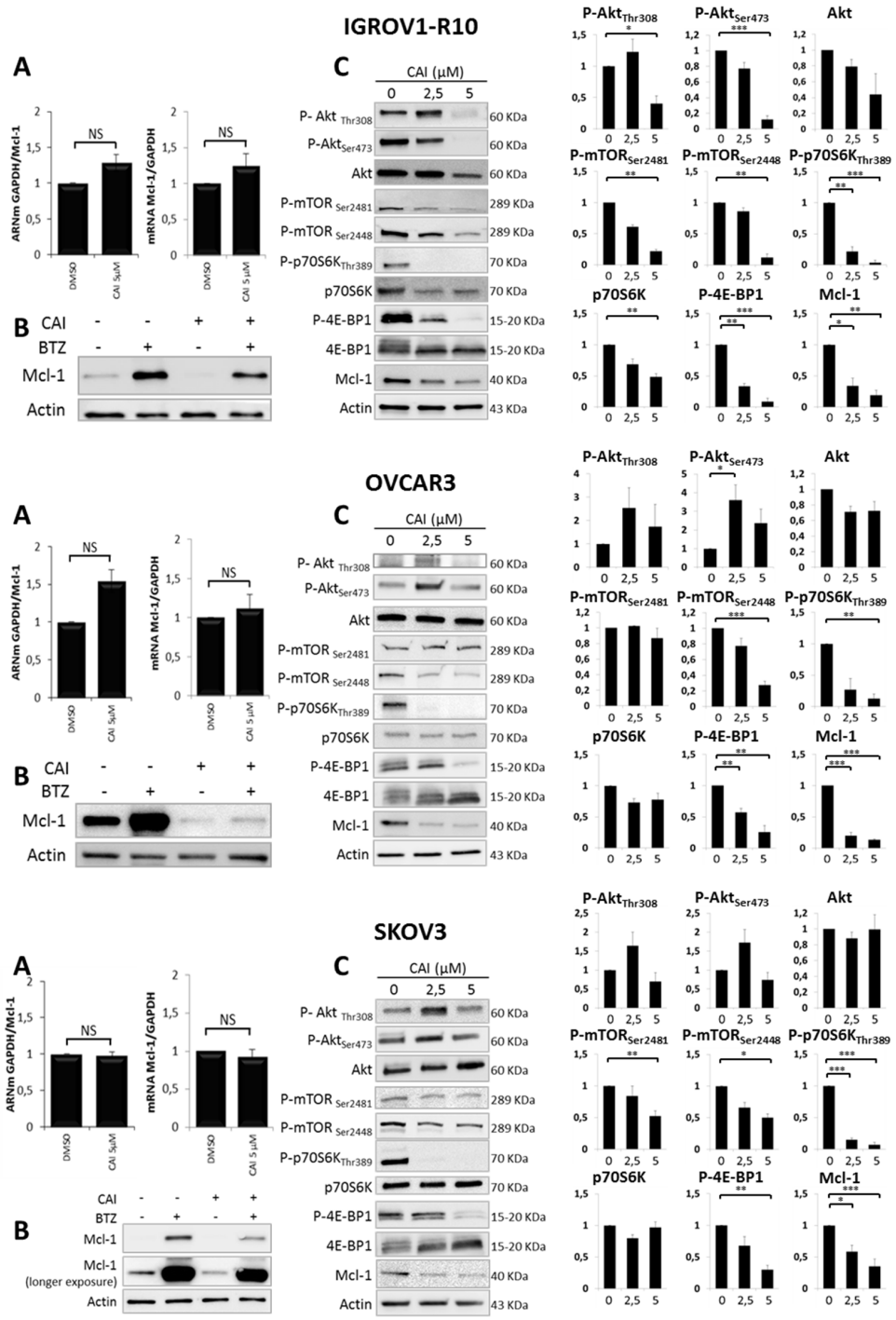

Figure 3: Mechanisms involved in CAI-induced Mcl-1 decrease. (A) Cells were treated or not (DMSO) with 5 µM CAI for 24h (left panel) and 48h (right panel) for IGROV1-R10 and 48h (left panel) and 72h (right panel) for OVCAR3 and SKOV3. Mcl-1 mRNA expression was assessed by real time quantitative RT-PCR. GAPDH was used as a housekeeping reference gene for normalization. Histograms represent the relative mRNA expression in treated cells normalized to that of control cells. Data are expressed as mean ± SEM of three independent experiments. Statistical differences were analyzed with a Student t-test: NS=non-significant; **(B)** Ovarian carcinoma cell lines were treated or not (DMSO) with 5 µM CAI for 48h for IGROV1-R10 and 72h for OVCAR3 and SKOV3. One hundred nM bortezomib were added for the last 24h of treatment. Mcl-1 expression was monitored by western blot; **(C)** Cells were treated with increasing dose of CAI for 48h for IGROV1-R10 and 72h for OVCAR3 and SKOV3. The effect of CAI treatment on the activation of the PI3K/Akt/mTOR pathway was analyzed by studying the protein expression of P-Akt (Ser473 and Thr308) and total Akt, P-mTORC1 (Ser2448) and P-mTORC2 (Ser2448), P-p70S6K (Thr389) and total p70S6K and P-4E-BP1 (Thr70) and total 4E-BP1 by western blot analysis. Protein levels (standardized based on actin) were determined by densitometry scanning with Image J software to generate the values shown in the bar graphs. Results are expressed as mean ± SEM. Statistical differences were analyzed with a Student t-test: $^{*}p< 0.05$, $^{**}p< 0.01$, $^{***}p< 0.001$ (n=3).

mTORC1 down-regulation and that further investigation was required to elucidate the molecular pathway involved.

YM48583, a SOCE inhibitor, down-regulates mTORC1 targets and Mcl-1

The involvement of SOCE in Mcl-1 down-regulation was confirmed using YM58483, a potent SOCE inhibitor [58]. We first verified that YM58483 was able to inhibit SOCE in our models. For this purpose, a "Ca^{2+} re-addition" protocol was used in the three cell lines pre-treated or not with YM53483. YM53483 did not inhibit calcium release triggered by thapsigargin in Ca^{2+} depleted medium but, as expected, it strongly reduced calcium entry *via* SOCE upon calcium reintroduction (Figure 4A). We then investigated whether YM58483 would mimic the effect of CAI on mTORC1 and Mcl-1 expression. For this purpose, we treated the cells for 48h (IGROV1-R10) and 72h (OVCAR3 and SKOV3) with YM53483 and assessed protein expression by western blot. As depicted in Figure 4B, YM53483 decreased phosphorylation of mTORC1(Ser2448) and its downstream targets, P-4E-BP1, P-p70S6K as well as Mcl-1 expression in the three cell lines tested. It did not down-regulate phosphorylation of Akt at residues Thr308 and Ser473, but through mTORC1 inhibition, released loops that re-induce their activation, as suggested by the literature [53]. Finally, YM58843 neither deactivated CamKII nor induced AMPK phosphorylation, strongly suggesting that inhibiting SOCE down-regulates Mcl-1 through mTORC1 inhibition (Supplemantary Data 2).

SOCE inhibition by CAI or YM58483 combined with anti-Bcl-x_L strategies leads to apoptosis in ovarian carcinoma

As Bcl-x_L and Mcl-1 cooperate to protect ovarian carcinoma cells from apoptosis, we next evaluated the efficacy of SOCE inhibitor/anti-Bclx_L strategies. First, we combined CAI with the BH3-mimetic ABT-737. As CAI-induced modulation of protein expression occurred more slowly than ABT-737-inhibited Bcl-x_L activity, cells were pretreated with CAI for 24h (IGROV1-R10 cells) or 48h (OVCAR3 and SKOV3 cells). Then the medium was supplemented with 1μM ABT-737 for the last 24h of treatment. As illustrated in Figure 5A, this combination led to a drastic decrease in cell viability of the three cell lines (about -75% for IGROV1-R10, -90% for OVCAR3 and -80% for SKOV3 cells). This observation was supported by the potent increase in sub-G1 peaks on flow cytometry (Figure 5B), as well as by the occurrence of PARP and caspase 3 cleavages on western blotting (Figure 5C). Moreover, combining CAI with siRNA targeting Bcl-x_L triggered massive apoptosis in the three cell lines, as suggested by caspase 3 and PARP cleavages (Supplementary Data 3).

We then evaluated the efficacy of the YM58483/ABT-737 combination in our carcinoma cell lines. Whereas YM58483 did not induce any cell death on its own at the concentrations tested, its combination with ABT-737 elicited a massive apoptosis, as displayed by the emergence of a strong sub-G1 peak and caspase 3 and PARP cleavages (Figure 5D and 5E). Altogether, these experiments illustrate that inhibiting SOCE strongly sensitizes chemoresistant ovarian cells to anti-Bcl-x_L strategies.

DISCUSSION

Despite remarkable progress in the understanding of apoptosis resistance, no alternative to platinum-based therapy has been approved yet for ovarian cancer. Hence, the development of new therapeutic strategies represents a crucial challenge for improving the present low survival rate of patients with advanced ovarian cancer. Several studies have shown that the anti-apoptotic proteins Bcl-x_L and Mcl-1 could constitute key targets for future therapeutic strategies [7, 59, 60]. In this line, we previously demonstrated that calcium signaling modulation targeted Mcl-1 translation and could be used to sensitize ovarian carcinoma to anti-Bcl-x_L strategies [13]. Our objective was then to test the effect of CAI, a calcium inhibitor used in clinical trials, on Mcl-1 expression and to evaluate its ability to sensitize ovarian carcinoma cells to anti-Bcl-x_L strategies.

CAI elicited an anti-proliferative effect in the three ovarian cancer cell lines tested, an effect consistent with several studies in other types of cancers at the same range of CAI concentrations and for the same durations of treatment [36, 37, 39, 61–63]. In our conditions, this effect was accompanied neither by a G2/M cell cycle arrest nor any apoptotic features, as observed in other cancer cell lines [63–66]. This could be due to the higher CAI concentrations (30 μM instead of 5 μM) or longer treatment times used in these studies. This could also explain why in our conditions Bcl-2 was not decreased upon CAI, as was the case in the MCF-7 breast cancer cell line [64]. In our hands, CAI potently inhibited Mcl-1 expression in ovarian carcinoma cells. Its effect cannot be ascribed to caspase 3 cleavage so its inhibitory effect is not a consequence of cell death, as already described [49]. This result is supported by our previous finding that Mcl-1 is decreased upon calcium signaling inhibition. To our knowledge, this is the first time that Mcl-1 has been found to be regulated by CAI in cancer cell lines.

CAI drastically inhibited SOC in our experimental models suggesting that it acts as a potent SOC inhibitor in ovarian carcinoma cells. SOC is one of the major calcium channels in non-excitable cells. These channels are composed of two sub-units, one belonging to the ER membrane (STIM-1) and the other to the cell plasma membrane (ORAI-1). Upon ER calcium depletion, these

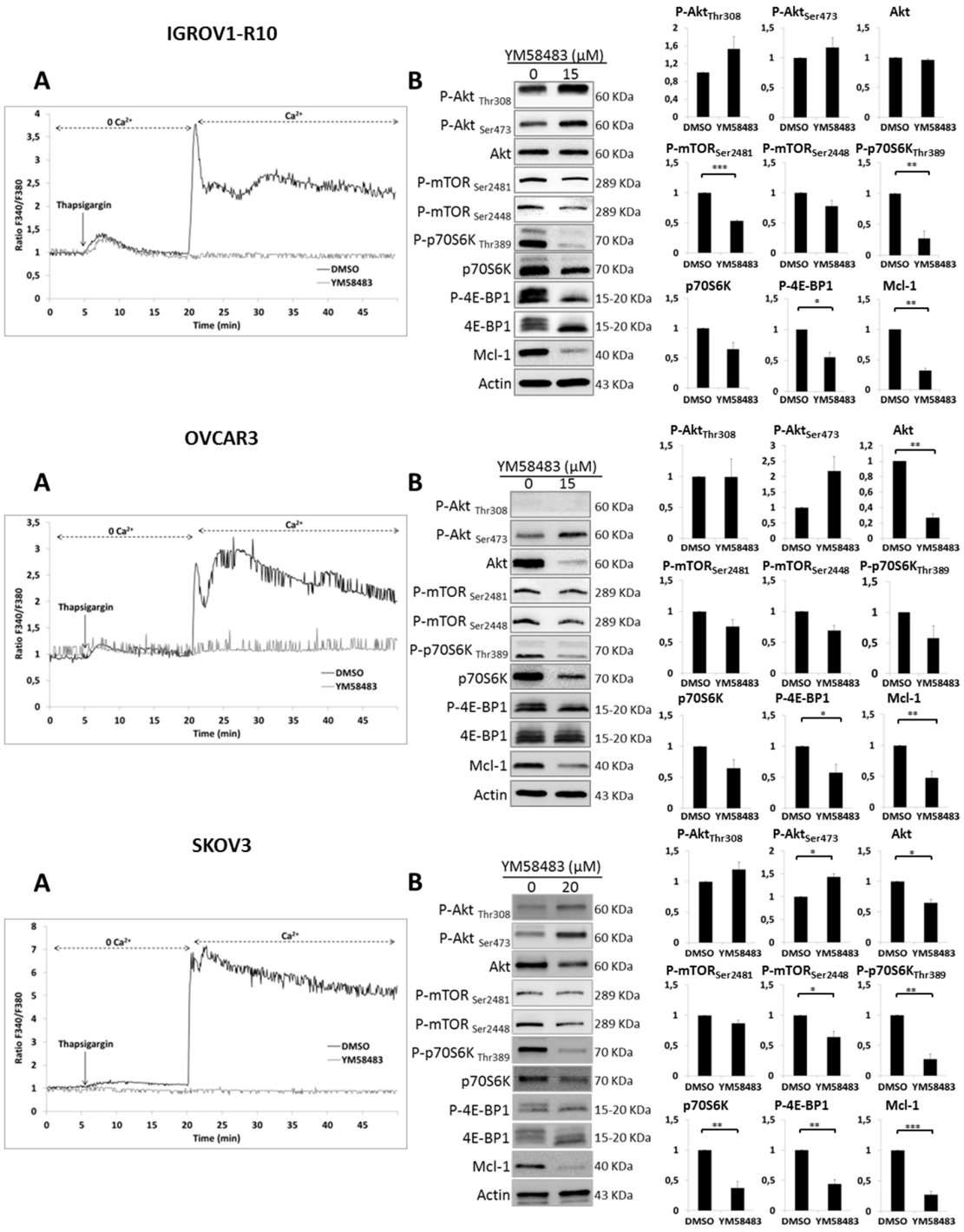

Figure 4: YM48583 blocks SOCE and inhibits mTORC1 targets and Mcl-1. (A) Effect of YM58483 on IP3R and SOC. Microspectrofluorimetry using Fura-2AM probe was performed in the three carcinoma cell lines IGROV1-R10, OVCAR3 and SKOV3 cells. During exposure to $0Ca^{2+}$, depletion of the intracellular stores was triggered by the addition of 2 µM thapsigargin to the bathing medium. Subsequent replenishment of 2 mM Ca^{2+} to the medium elicited a rise in $[Ca^{2+}]_i$ due to Ca^{2+} influx through open store-operated channels. Black tracings depict the representative changes in $[Ca^{2+}]_i$ recorded from DMSO treated cells and grey tracings depict the representative changes in $[Ca^{2+}]_i$ recorded from cells pre-treated 1h with 15 µM for IGROV1-R10 and OVCAR3 cells or 20 µM for SKOV3 cells (data are representative of three independent experiments). **(B)** Effect of YM58483 on Akt/mTORC1 pathway. Cells were treated with YM58483 (15 µM for 48h for IGROV1-R10 cells, 15 µM for 72h for OVCAR3 cells and 20 µM for 72h for SKOV3 cells). The effect of YM58483 treatment on the activation of the PI3K/Akt/mTOR pathway was analyzed by studying the protein expression of P-Akt (Ser473 and Thr308) and total Akt, P-mTORC1 (Ser2448) and P-mTORC2 (Ser2448), P-p70S6K (Thr389) and total p70S6K and P-4E-BP1 (Thr70) and total 4E-BP1 by western blot analysis. Protein levels (standardized based on actin) were determined by densitometry scanning with Image J software to generate the values shown in the bar graphs. Results are expressed as mean ± SEM. Statistical differences were analyzed with a Student t-test: $^{*}p< 0.05$, $^{**}p< 0.01$, $^{***}p< 0.001$ (n=3).

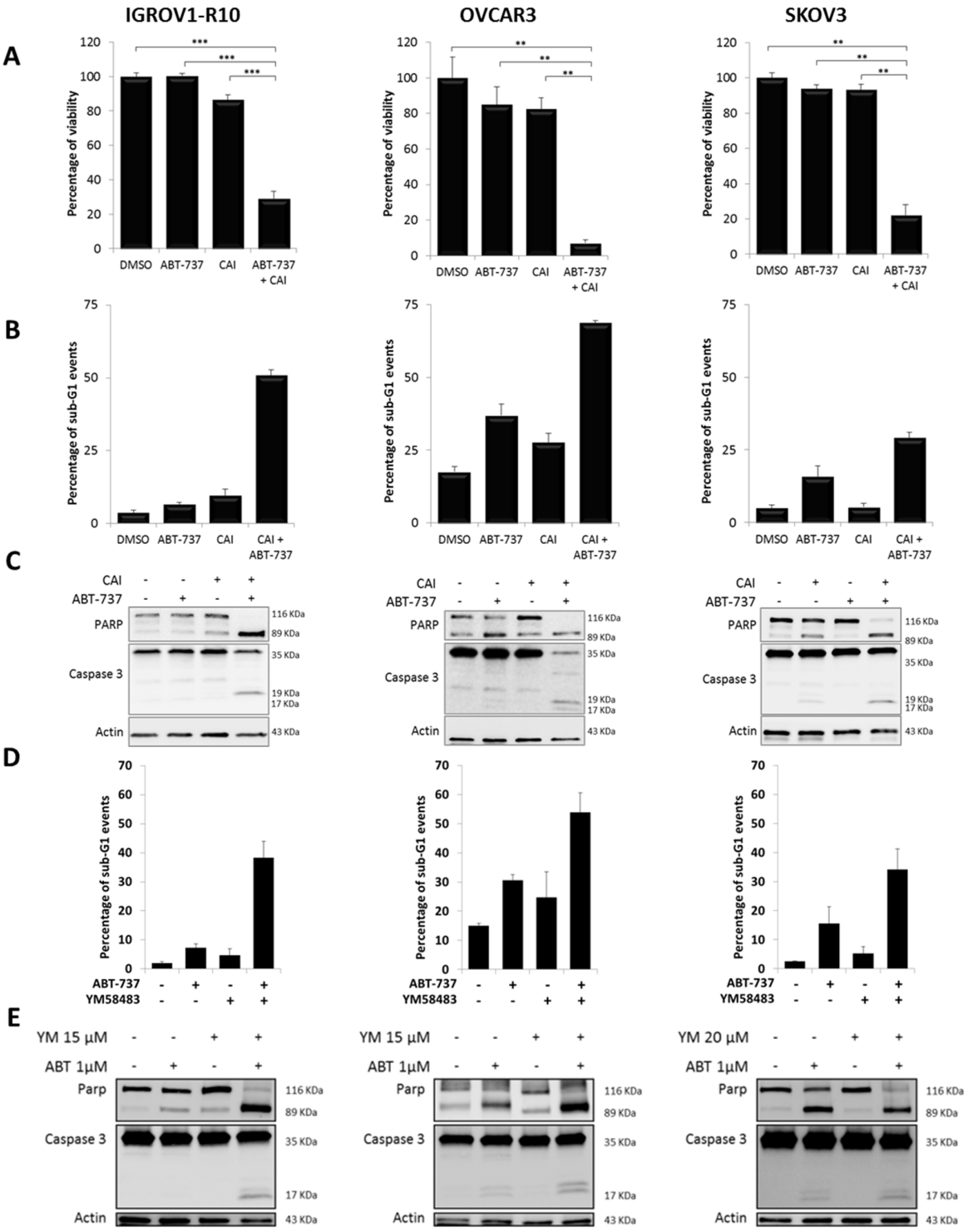

Figure 5: CAI or YM58483 combined with ABT-737 leads to apoptosis in ovarian carcinoma. Cells were treated or not (DMSO) with 5 µM CAI for 48h for IGROV1-R10 or 72h for OVCAR3 and SKOV3, and 1 µM ABT-737 was added 24h before the end of the experiment. **(A)** Cell viability was assessed by trypan blue exclusion. Data are expressed as mean ± SEM of three independent experiments. Statistical differences were analyzed with a Wilcoxon test: $^{*}p< 0.05$, $^{**}p< 0.01$, $^{***}p< 0.001$. **(B)** Sub-G1 events were studied by flow cytometry. Data are expressed as mean ± SEM of three independent experiments. **(C)** PARP and caspase 3 cleavages were assessed by western blot. **(D)** YM58483 sensitizes ovarian carcinoma cells to ABT-737. Cells were treated with YM58483 (15 µM for 48h for IGROV1-R10 cells, 15 µM for 72h for OVCAR3 cells and 20 µM for 72h for SKOV3 cells). One micromolar ABT-737 was added for the last 24h hours of treatment. Sub-G1 events were studied by flow cytometry. **(E)** YM58483 sensitizes ovarian carcinoma cells to ABT-737. Cells were treated with YM58483 (15 µM for 48h for IGROV1-R10 cells, 15 µM for 72h for OVCAR3 cells and 20 µM for 72h for SKOV3 cells). One micromolar ABT-737 was added for the last 24h hours of treatment. PARP and caspase 3 cleavages were assessed by western blot.

subunits interact with each other leading to a calcium influx from extracellular compartments in order to refill cytoplasm and ER stocks subsequently. Our finding is supported by other studies showing that CAI inhibits SOC in HEK293 [40], colon carcinoma cells [33], human endothelial cells [34] and endothelial progenitor cells isolated from patients [39]. In contrast, it did not significantly inhibit calcium release from IP3 receptor induced by thapsigargin, as observed in HUVEC and Rat-1 cells [67].

CAI-induced Mcl-1 inhibition did not require transcriptional events and its effect was not reversed by proteasomal inhibition, implying that post-translational events were not involved in the Mcl-1 decrease. The Mcl-1 down-regulation we evidenced may be attributed to translational events, as CAI strongly repressed P-4E-BP1, which is known to control Mcl-1 protein expression [11, 12]. This result corroborates those obtained with the calcium chelator BAPTA-AM in the same experimental models. Indeed, we previously found that BAPTA-AM treatment led to down-regulation of Mcl-1, which was counteracted by the overexpression of the 4E-BP1 target (eiF4E) [13].

Calcium can control the PI3K-AKT-mTOR pathway at several levels". Indeed, calcium/calmodulin(CaM) complex has been shown to activate P-Akt(Ser473), and subsequently mTORC1, through CaMKII activation in B lymphocytes [30]. Consistent with this finding, SKF-96365, another SOCE inhibitor, inhibited the calcium/CaMKIIγ/Akt/mTORC1-mediated pathway in colorectal cancer cells [55]. However, CAI did not inhibit the activation of CaMKII in our carcinoma cell model. Other studies reported that calcium could activate this survival pathway through a calcium/CaM/CaMKK2 complex that bound to and activated P-Akt(Thr308) in ovarian carcinoma cells [68]. Nevertheless, in our conditions, P-Akt(308) was not down-regulated by CAI. Furthermore, since one of the major targets of CamKK2 is AMPK protein, it could be hypothesized that decreasing calcium could lead to a down-regulation in the CamKK2/AMPK pathway and consequently to an up-regulation of mTORC1, as previously described [69, 70]. Nonetheless, the contrary result we obtained implies that calcium/CamKK2 is not the main pathway targeted by CAI and that CamKK2 is not involved in mTORC1 and Mcl-1 down-regulation.

Our results strongly suggest that SOCE inhibition by CAI impaired PI3K/Akt/mTOR by inactivating mTORC1, as evidenced by the potent inhibition of mTORC1(Ser2448), p70S6K and 4E-BP1 protein phosphorylation. This effect was confirmed by the appearance of a transient upregulation of P-Akt(308) triggered by a compensatory feedback upon mTORC1 inhibition [54]. It is noteworthy that in OVCAR3 and SKOV3 cells, this feedback loop also led to a transient up-regulation of P-Akt(473) due to the release of the inhibitory effect of mTORC1 on mTORC2, which phosphorylates Akt(473). However, this effect was not observed in the IGROV1-R10 cell line, suggesting that mTORC1 inhibition could lead to independent regulation of the two phosphorylation sites. This conclusion is supported by several studies showing that Akt(308) and Akt(473) reactivation depends on the cellular context [53].

The hypothesis that calcium could play an important role in the regulation of mTOR signaling was evidenced by the need for calcium to activate p70S6K [24–26]. Thereafter, the role of calcium and calmodulin in mTORC1 activation was observed in a context of amino acid starvation [27]. Finally, lysosomal calcium was demonstrated to activate mTORC1 by inducing an association of calmodulin with mTORC1; the authors suggested that mTORC1 could be regarded as an "atypical calmodulin-dependent kinase" [31]. They also showed that although calcium signaling repression inhibited both mTORC1 and mTORC2, mTORC1 was inhibited at lower concentrations than those at which mTORC2 was inhibited. This supports our finding that calcium inhibition could down-regulate mTORC1 activation independently of its action on Akt(473).

To consolidate our findings with CAI, we then tested the effect of YM-58483, a well-known SOC inhibitor, on SOC channels and Akt/mTOR activation in ovarian carcinoma cells. As expected, YM58483 strongly down-regulated SOCE but had no impact on calcium release from IP3R, thereby confirming its action as an SOCE inhibitor. Moreover, its effect on the PI3K/Akt/mTOR pathway mimicked that obtained with CAI. YM85483 potently inhibited mTORC1 activation, leading to compensatory feedback loops on Akt and to inhibition of the mTORC1 downstream targets P-p70S6K and P-4E-BP1. Finally, YM-58483 also drastically inhibited Mcl-1 expression, so it is highly likely that Mcl-1 is a target for SOCE inhibitors. The link between SOCE and the expression of Bcl-2 family members had already been pointed out by a few studies but led to divergent conclusions. On the one hand, a constitutively active mutated STIM-1 led to induction of Mcl-1 transcription in HEK293; on the other hand, ORAI1 knock-down promoted Mcl-1 and inhibited Noxa expressions leading to survival of activated murine T cells [71, 72]. These discrepancies are probably inherent to the experimental model so further investigations are required to unravel the molecular pathway involved.

SOC play a crucial role in tumor development and accumulating evidence suggests that their activation is involved in cancer progression. First, they are differentially expressed in malignant cells and STIM1 and ORAI1 were found to be more strongly expressed in hepatoma tissues than in pre-cancerous tissues or non-tumoral tissues from the same patients [73, 74]. Second, they were demonstrated to play a crucial role in the invasion of glioblastoma cells [75], in angiogenesis by

endothelial progenitor cells isolated from tumoral patients [39] and in migration and metastasis of breast cancer [76] and cervical cancer cells [77]. Finally, SOCE inhibition sensitized various cancer cells to apoptosis. It potentiated 5-FU-induced inhibition of the PI3K/AKT/mTOR pathway and synergized with 5-FU to induce cell death [74]. Furthermore, SKF96365 potentiated the anticancer effect of hydroxychloroquine in a mouse xenograft model through calcium/CaMKIIγ/AKT/mTOR inhibition [55]. Finally, in ovarian carcinoma, STIM and ORAI1 were found to be more strongly expressed in cisplatin-resistant cells (A2780cis) than in their sensitive counterpart (A2780), and the combination of cisplatin with 2-APB, a SOC inhibitor, restored A2780cis sensitivity [78]. Taken together, these findings suggest that SOC could provide interesting predictive factors of cancer progression and that targeting them could sensitize carcinoma cells to apoptosis.

On the basis of these results and those we previously obtained with BAPTA-AM [13], we combined CAI or YM58483 with the BH3-mimetic ABT-737 and found that they strongly sensitized ovarian carcinoma cell lines to anti-Bcl-x_L strategies in the three cell lines tested. Because our experimental model is dependent on Mcl-1 and Bcl-x_L to survive, the massive cell death we observed with SOC inhibitors and an inhibitor of Bcl-x_L strongly suggests that Mcl-1 expression is regulated by SOC channels. Moreover, the anti-tumoral effect of this combination could explain the mild efficacy of CAI when it was used as a single agent in clinical trials, as the sole inhibition of Mcl-1 is not sufficient to induce apoptosis in ovarian cancer [45]. CAI has been tested in combination with several compounds and has been shown to potentiate the anti-tumoral activity of sorafenib [63], LM-1685, a celecoxib analogue [79], 2-deoxyglucose [80] and Temozolomide [48]. In this recent phase IB clinical trial conducted in cohorts of recurrent or newly diagnosed glioblastoma, patients were treated with increasing doses of the oral derivative of this calcium channel blocker (Carboxyamidotriazole orotate - CTO) in combination with temozolomide ± radiotherapy. The results showed, on the one hand, that CTO is well tolerated by patients confirming results observed in previous clinical trials and on the other hand that treatment was effective on these aggressive cancers. This clinical trial showed that CAI has to be combined with another anti-neoplastic molecule in order to have a good therapeutic efficacy and it should be noted that the best clinical responses were obtained for tumors with EGFR amplification as well as mutations of the Akt / mTOR, PTEN and PI3KCA pathway [48]. Therefore these results strongly support all those we have obtained in ovarian cancer.

To our knowledge, this is the first time that CAI has been shown to sensitize cancerous cells to Bcl-x_L inhibitors. Furthermore, this is the first report of SOC inhibitors sensitizing chemoresistant ovarian cells to anti-Bcl-x_L strategies. This offers interesting perspectives for the clinical use of ABT-263 (Navitoclax, the orally available ABT-737 analogue). Due to its ability to antagonize the survival function of Bcl-x_L in platelets, it triggers thrombocytopenia, which is its major dose-limiting side-effect. As CAI synergizes with ABT-737, it might allow a dose reduction of ABT-263, thereby alleviating the BH3-mimetic side-effect.

In conclusion, we show that CAI has an anti-proliferative effect on ovarian cell lines and that it inhibits Mcl-1 expression through SOCE/mTORC1 inhibition, which leads to a strong sensitization of ovarian carcinoma to anti-Bcl-x_L strategies. We hypothesize that CAI, *via* its action on SOCE and Mcl-1, could extend the therapeutic arsenal for ovarian cancer treatment if combined pertinently. As SOC are known to interact with the frequently deregulated PI3K/Akt/mTOR pathway, they could offer a relevant target to overcome apoptosis resistance in ovarian carcinoma.

MATERIALS AND METHODS

Cell culture

The human platinum-resistant ovarian carcinoma cell lines IGROV1-R10, OVCAR3, and SKOV3 were used. IGROV1-R10 was established as described previously (34) from the IGROV1 cell line, kindly provided by Dr. Jean Bénard (Institut Gustave Roussy, Villejuif, France). OVCAR3 and SKOV3 were obtained from the ATCC. The cell lines were authenticated in April 2016 by Microsynth who compared their STR profiles with the ATCC database. They were grown in RPMI1640 medium (Gibco) supplemented with 2 mM Glutamax™, 25 mM HEPES, 10% FBS (Gibco) and 33 mM sodium bicarbonate and were maintained in a 5% CO_2 humidified atmosphere at 37°C.

Reagents

CAI, YM58493, thapsigargin were provided by Tocris (R&D Systems). ABT-737 was supplied by Selleckem and Bortezomib (Velcade®) was supplied by Millennium Pharmaceuticals. Fura-2AM was purchased from Thermo Fisher Scientific. These compounds were commonly stored as stock solutions in DMSO at -20°C.

Proliferation analysis

Cell number and viability were estimated by a semi-automated image-based cell analyzer (Cedex XS Analyzer, Roche Applied Science, Meylan, France) using the Trypan blue exclusion method.

Cell cycle analysis by flow cytometry

Adherent and floating cells were pooled, washed with phosphate-buffered saline (PBS 1X) and fixed with

ethanol 70%. Cells were then centrifuged at 2000 rpm for 5 min and incubated for 30 min at 37°C in PBS 1X, to allow the release of low-molecular weight DNA. Cell pellets were stained with propidium iodide using the DNA Prep Coulter Reagent Kit (Beckman-Coulter). Samples were analyzed with a Gallios flow cytometer (Beckman Coulter).

Western immunoblotting

Cells were rinsed with ice-cold PBS 1X and lysed in lysis buffer (15 mM HEPES, 50 mM KCl, 10 mM NaCl, 1 mM $MgCl_2$, 0.25% glycerol, 0.5% laurylmaltoside, 5 µM GDP, 1 µM microcystin (Enzo Life Sciences), 1 mM sodium orthovanadate and cOmplete Protease Inhibitor Cocktail (Sigma-Aldrich/Roche). After centrifugation, proteins were quantified using the Bradford assay (Bio-Rad, CA). Thirty micrograms of proteins were separated by SDS–PAGE (Biorad) and transferred to PVDF membranes (Millipore). After blocking, membranes were incubated overnight at 4°C with the following primary antibodies: Bcl-2 (#M0887, DAKO), actin (MAB1501, Merck Millipore), Mcl-1 (#5453), Bcl-x_L (#2764), PARP(#9542), caspase-3 (#9662), P-Akt (Thr308; #13038), P-Akt (Ser473; #4060), Akt (#9272), P-4E-BP1 (Thr70; #4370), 4E-BP1 (#9644), P-p70S6K (Thr389; #9205) and p70S6K (#9202), P-mTOR (Ser2448 ; #5536), P-mTOR (Ser2481; #2974), p-CamKII (Thr286; #12716), p-AMPK (Ser485; #4184), AMPK (#2532) (Cell Signaling Technology). Membranes were then incubated with the appropriate horseradish peroxidase-conjugated secondary antibodies (GE Healthcare). Revelation was done using Clarity Western ECL (Biorad). Western blots shown are from one experiment representative of at least three independent experiments and cell lysates. Signals were quantified by pixel densitometry using the ImageJ software.

RNA extraction and real-time quantitative reverse transcription PCR (qRT-PCR)

Total RNA was isolated from ovarian carcinoma cell lines using Trizol (Invitrogen, Life Technologies). RNA quantity and quality were assessed using the NanoDropTM 2000 spectrophotometer (Thermo Scientific). The first strand cDNA was synthesized using the Omniscript reverse transcriptase kit (Qiagen) with random hexamers. cDNA (25 ng) were combined with 10 µmol/l of each forward and reverse primer, 50 µmol/l of the Taq-Man® probe and TaqMan® Fast Universal PCR Master Mix (Applied Biosystems) in a 20 µl final reaction volume. Corresponding custom inventoried (ID: Hs00172036_m1 for Mcl-1 and Hs99999905_m1 for GAPDH) TaqMan® Gene Expression Assays were used (Applied Biosystems). All PCR amplification reactions were carried out in triplicate and detection was done on an Applied ABI Prism 7500 Fast PCR system (Applied Biosystems). GAPDH was used as a housekeeping reference gene for normalization.

siRNA transfection

PAGE-purified siRNAs were synthesized and annealed by the Eurogentec Company. Specific double-stranded 21 nt RNA oligonucleotides forming a 19 bp duplex core with 2 nt 3' overhangs were used to silence Bcl-x_L (5’ auuggugagucggaucgca-3’, noted siXL). siGENOME Non-Targeting siRNA Pool#1 (noted siCT) was purchased from Dharmacon. siRNA duplexes were transfected using the INTERFERin™ transfection reagent according to the manufacturer's instructions (Polyplus-Transfection). Briefly, cells were seeded in 25 cm^2 flasks to reach 30–50% of confluence at the time of transfection. The transfection reagent and the siRNAs were mixed and complex formation was allowed to proceed for 15 min at room temperature before application to cells. After the indicated time, cells were trypsinized and washed with ice-cold PBS 1X before analysis.

Calcium imaging

Intracellular calcium concentration variations were analyzed by microspectrofluorimetry using the Ca^{2+}-sensitive probe Fura-2-AM as described previously [81]. Briefly, ovarian carcinoma cells were incubated at 37 °C in HBBSS buffer (116 mM NaCl; 5.4 mM KCl; 0.8 mM $MgSO_4$; 12 mM HEPES; 0.34 mM NaH_2PO_4; 25 mM $NaHCO_3$; 5.5 mM D-glucose; 10 µM Glycine; 1.8 mM $CaCl_2$; pH 7.4) supplemented with 10 µM Fura-2-AM (#F1201 Thermofisher Scientific) for 45 min. Following probe loading, cells were treated or not by 5 µM CAI for 45 min. Then they were placed in a recording chamber mounted on the stage of an epifluorescence inverted microscope (Lieca DMI 6000 B) equipped with a 150 W xenon high stability lamp and a Leica 40 ×, 1.3 numerical aperture epifluorescence oil immersion objective (Wetzlar, Germany). Fura-2AM-loaded cells were treated with 2 µM thapsigargin in HBBSS without $CaCl_2$ ($0Ca^{2+}$) to trigger calcium efflux from the RE. To test SOCE, calcium was reintroduced in the medium by using classical HBBSS ($+Ca^{2+}$). During the acquisition, cells were irradiated alternately with 340 and 380 nm light, and fluorescence from the trapped dye was measured at 510 nm. The ratio of fluorescence intensities recorded after excitation at 340 nm (F340) and at 380 nm (F380) was used to estimate intracellular calcium concentrations ($[Ca^{2+}]_i$) and was acquired every 5 seconds with a digital CMOS camera (Hamamatsu, ORCA-Flash2.8 C11440-10C). The monochromator and the photometers allow emission and detection of fluorescence from ~12 cells in the field of view. Data analysis was performed using MM fluor software (Universal Imaging Corporation).

Statistical analysis

The values are presented as means ± S.E.M. for at least three independent experiments. Student's *t*-test was used for statistical analysis of densitometry graphs and Wilcoxon test was used for analysis of percentage of viable cells. Differences were considered statistically different if $p<0.05$ (*); $p<0.01$ (**); $p<0.001$ (***).

Abbreviations

4E-BP1: eukaryotic translation initiation factor 4E (eIF4E)-binding protein; AMPK: AMP-activated protein kinase; $[Ca^{2+}]_i$ intracytosolic calcium concentration; CAI: Carboxyamidotriazole; CaM: Calmodulin; CamKII: Ca 2+ /calmodulin-dependent protein kinase II; CamKK2: Calcium/calmodulin-dependent protein kinase kinase 2; IP3R: Inositol Trisphosphate Receptor; mTORC1/2: mammalian Target Of Rapamycin Complex 1 / 2; p70S6K: p70 S6 kinase; PARP: Poly(ADP-ribosyl) polymerase; PI3K: phosphatidylinositol 3-kinase; STIM: stromal interaction molecule, ORAI: calcium release-activated calcium modulator; PDX: Patient derived xenograft; SERCA: sarco/endoplasmic reticulum Ca^{2+}-ATPase; SOCE: Store-Operated Calcium Entry; TRP: Transient Receptor Potential.

ACKNOWLEDGMENTS

The research was supported by the Ligue Contre le Cancer (Comité départemental de l'Orne). Marie-Laure Bonnefond and Romane Florent were funded by a grant from Normandy Regional Council and Marie-Laure Bonnefond was also funded by Accord Healthcare Inc. We thank Marilyne Guillamin (Flow Cytometry Core Facility, SF 4206 ICORE of University of Caen Normandy) for technical assistance. We thank Dr Nicolas Vigneron (INSERM U1086, ANTICIPE) for his advice about statistical data, Dr Marie Villedieu (INSERM U1086, ANTICIPE) for her careful reading and M. Ray Cooke for English editing.

CONFLICTS OF INTEREST

The authors declare no conflicts of interest.

REFERENCES

1. Siegel RL, Miller KD, Jemal A. Cancer Statistics, 2017. CA Cancer J Clin. 2017; 67:7-30.
2. Ledermann JA, Raja FA, Fotopoulou C, Gonzalez-Martin A, Colombo N, Sessa C, and ESMO Guidelines Working Group. Newly diagnosed and relapsed epithelial ovarian carcinoma: ESMO Clinical Practice Guidelines for diagnosis, treatment and follow-up. Ann Oncol. 2013 (Suppl 6); 24:vi24–32.
3. Hanahan D, Weinberg RA. Hallmarks of cancer: the next generation. Cell. 2011; 144:646–74.
4. Juin P, Geneste O, Gautier F, Depil S, Campone M. Decoding and unlocking the BCL-2 dependency of cancer cells. Nat Rev Cancer. 2013; 13:455–65.
5. Gloaguen C, Voisin-Chiret AS, Sopkova-de Oliveira Santos J, Fogha J, Gautier F, De Giorgi M, Burzicki G, Perato S, Pétigny-Lechartier C, Simonin-Le Jeune K, Brotin E, Goux D, N'Diaye M, et al. First evidence that oligopyridines, α-helix foldamers, inhibit Mcl-1 and sensitize ovarian carcinoma cells to Bcl-xL-targeting strategies. J Med Chem. 2015; 58:1644–68.
6. Simonin K, N'Diaye M, Lheureux S, Loussouarn C, Dutoit S, Briand M, Giffard F, Brotin E, Blanc-Fournier C, Poulain L. Platinum compounds sensitize ovarian carcinoma cells to ABT-737 by modulation of the Mcl-1/Noxa axis. Apoptosis. 2013; 18:492–508.
7. Brotin E, Meryet-Figuière M, Simonin K, Duval RE, Villedieu M, Leroy-Dudal J, Saison-Behmoaras E, Gauduchon P, Denoyelle C, Poulain L. Bcl-XL and MCL-1 constitute pertinent targets in ovarian carcinoma and their concomitant inhibition is sufficient to induce apoptosis. Int J Cancer. 2010; 126:885–95.
8. Kassem L, Abdel-Rahman O. Targeting mTOR pathway in gynecological malignancies: biological rationale and systematic review of published data. Crit Rev Oncol Hematol. 2016; 108:1–12.
9. Mabuchi S, Kuroda H, Takahashi R, Sasano T. The PI3K/AKT/mTOR pathway as a therapeutic target in ovarian cancer. Gynecol Oncol. 2015; 137:173–79.
10. Bell D, Berchuck A, Birrer M, Chien J, Cramer DW, Dao F, Dhir R, DiSaia P, Gabra H, Glenn P, Godwin AK, Gross J, Hartmann L, et al, and Cancer Genome Atlas Research Network. Integrated genomic analyses of ovarian carcinoma. Nature. 2011; 474:609–15.
11. Hsieh AC, Costa M, Zollo O, Davis C, Feldman ME, Testa JR, Meyuhas O, Shokat KM, Ruggero D. Genetic dissection of the oncogenic mTOR pathway reveals druggable addiction to translational control via 4EBP-eIF4E. Cancer Cell. 2010; 17:249–61.
12. Mills JR, Hippo Y, Robert F, Chen SM, Malina A, Lin CJ, Trojahn U, Wendel HG, Charest A, Bronson RT, Kogan SC, Nadon R, Housman DE, et al. mTORC1 promotes survival through translational control of Mcl-1. Proc Natl Acad Sci USA. 2008; 105:10853–58.
13. Bonnefond ML, Lambert B, Giffard F, Abeilard E, Brotin E, Louis MH, Gueye MS, Gauduchon P, Poulain L, N'Diaye M. Calcium signals inhibition sensitizes ovarian carcinoma cells to anti-Bcl-xL strategies through Mcl-1 down-regulation. Apoptosis. 2015; 20:535–50.
14. Anderson GR, Wardell SE, Cakir M, Crawford L, Leeds JC, Nussbaum DP, Shankar PS, Soderquist RS, Stein EM, Tingley JP, Winter PS, Zieser-Misenheimer EK, Alley HM, et al. PIK3CA mutations enable targeting of a breast tumor

dependency through mTOR-mediated MCL-1 translation. Sci Transl Med. 2016; 8:369ra175.

15. Faber AC, Li D, Song Y, Liang MC, Yeap BY, Bronson RT, Lifshits E, Chen Z, Maira SM, García-Echeverría C, Wong KK, Engelman JA. Differential induction of apoptosis in HER2 and EGFR addicted cancers following PI3K inhibition. Proc Natl Acad Sci USA. 2009; 106:19503–08.
16. Jebahi A, Villedieu M, Pétigny-Lechartier C, Brotin E, Louis MH, Abeilard E, Giffard F, Guercio M, Briand M, Gauduchon P, Lheureux S, Poulain L. PI3K/mTOR dual inhibitor NVP-BEZ235 decreases Mcl-1 expression and sensitizes ovarian carcinoma cells to Bcl-xL-targeting strategies, provided that Bim expression is induced. Cancer Lett. 2014; 348:38–49.
17. Zervantonakis IK, Iavarone C, Chen HY, Selfors LM, Palakurthi S, Liu JF, Drapkin R, Matulonis U, Leverson JD, Sampath D, Mills GB, Brugge JS. Systems analysis of apoptotic priming in ovarian cancer identifies vulnerabilities and predictors of drug response. Nat Commun. 2017; 8:365.
18. Berridge MJ, Lipp P, Bootman MD. The versatility and universality of calcium signalling. Nat Rev Mol Cell Biol. 2000; 1:11–21.
19. Prevarskaya N, Ouadid-Ahidouch H, Skryma R, Shuba Y. Remodelling of Ca2+ transport in cancer: how it contributes to cancer hallmarks? Philos Trans R Soc Lond B Biol Sci. 2014; 369:20130097.
20. Cui C, Merritt R, Fu L, Pan Z. Targeting calcium signaling in cancer therapy. Acta Pharm Sin B. 2017; 7:3–17.
21. Monteith GR, Prevarskaya N, Roberts-Thomson SJ. The calcium-cancer signalling nexus. Nat Rev Cancer. 2017; 17:367–80.
22. Monteith GR, Davis FM, Roberts-Thomson SJ. Calcium channels and pumps in cancer: changes and consequences. J Biol Chem. 2012; 287:31666–73.
23. Prevarskaya N, Skryma R, Shuba Y. Targeting Ca^{2+} transport in cancer: close reality or long perspective? Expert Opin Ther Targets. 2013; 17:225–41.
24. Conus NM, Hemmings BA, Pearson RB. Differential regulation by calcium reveals distinct signaling requirements for the activation of Akt and p70S6k. J Biol Chem. 1998; 273:4776–82.
25. Hannan KM, Thomas G, Pearson RB. Activation of S6K1 (p70 ribosomal protein S6 kinase 1) requires an initial calcium-dependent priming event involving formation of a high-molecular-mass signalling complex. Biochem J. 2003; 370:469–77.
26. Graves LM, He Y, Lambert J, Hunter D, Li X, Earp HS. An intracellular calcium signal activates p70 but not p90 ribosomal S6 kinase in liver epithelial cells. J Biol Chem. 1997; 272:1920–28.
27. Gulati P, Gaspers LD, Dann SG, Joaquin M, Nobukuni T, Natt F, Kozma SC, Thomas AP, Thomas G. Amino acids activate mTOR complex 1 via Ca2+/CaM signaling to hVps34. Cell Metab. 2008; 7:456–65.
28. Mercan F, Lee H, Kolli S, Bennett AM. Novel role for SHP-2 in nutrient-responsive control of S6 kinase 1 signaling. Mol Cell Biol. 2013; 33:293–306.
29. Zhou X, Lin DS, Zheng F, Sutton MA, Wang H. Intracellular calcium and calmodulin link brain-derived neurotrophic factor to p70S6 kinase phosphorylation and dendritic protein synthesis. J Neurosci Res. 2010; 88:1420–32.
30. Ke Z, Liang D, Zeng Q, Ren Q, Ma H, Gui L, Chen S, Guo M, Xu Y, Gao W, Zhang S, Chen L. hsBAFF promotes proliferation and survival in cultured B lymphocytes via calcium signaling activation of mTOR pathway. Cytokine. 2013; 62:310–21.
31. Li RJ, Xu J, Fu C, Zhang J, Zheng YG, Jia H, Liu JO. Regulation of mTORC1 by lysosomal calcium and calmodulin. eLife. 2016; 5:5.
32. Antoniotti S, Fiorio Pla A, Pregnolato S, Mottola A, Lovisolo D, Munaron L. Control of endothelial cell proliferation by calcium influx and arachidonic acid metabolism: a pharmacological approach. J Cell Physiol. 2003; 197:370–78.
33. D'Amato M, Flugy AM, Alaimo G, Bauder B, Kohn EC, De Leo G, Alessandro R. Role of calcium in E-selectin induced phenotype of T84 colon carcinoma cells. Biochem Biophys Res Commun. 2003; 301:907–14.
34. Faehling M, Kroll J, Föhr KJ, Fellbrich G, Mayr U, Trischler G, Waltenberger J. Essential role of calcium in vascular endothelial growth factor A-induced signaling: mechanism of the antiangiogenic effect of carboxyamidotriazole. FASEB J. 2002; 16:1805–07.
35. Fiorio Pla A, Grange C, Antoniotti S, Tomatis C, Merlino A, Bussolati B, Munaron L. Arachidonic acid-induced Ca2+ entry is involved in early steps of tumor angiogenesis. Mol Cancer Res. 2008; 6:535–45.
36. Moody TW, Chiles J, Moody E, Sieczkiewicz GJ, Kohn EC. CAI inhibits the growth of small cell lung cancer cells. Lung Cancer. 2003; 39:279–88.
37. Wu Y, Palad AJ, Wasilenko WJ, Blackmore PF, Pincus WA, Schechter GL, Spoonster JR, Kohn EC, Somers KD. Inhibition of head and neck squamous cell carcinoma growth and invasion by the calcium influx inhibitor carboxyamido-triazole. Clin Cancer Res. 1997; 3:1915–21.
38. Enfissi A, Prigent S, Colosetti P, Capiod T. The blocking of capacitative calcium entry by 2-aminoethyl diphenylborate (2-APB) and carboxyamidotriazole (CAI) inhibits proliferation in Hep G2 and Huh-7 human hepatoma cells. Cell Calcium. 2004; 36:459–67.
39. Lodola F, Laforenza U, Bonetti E, Lim D, Dragoni S, Bottino C, Ong HL, Guerra G, Ganini C, Massa M, Manzoni M, Ambudkar IS, Genazzani AA, et al. Store-operated Ca2+ entry is remodelled and controls *in vitro* angiogenesis in endothelial progenitor cells isolated from tumoral patients. PLoS One. 2012; 7:e42541.
40. Mignen O, Brink C, Enfissi A, Nadkarni A, Shuttleworth TJ, Giovannucci DR, Capiod T. Carboxyamidotriazole-induced

inhibition of mitochondrial calcium import blocks capacitative calcium entry and cell proliferation in HEK-293 cells. J Cell Sci. 2005; 118:5615–23.

41. Azad N, Perroy A, Gardner E, Imamura CK, Graves C, Sarosy GA, Minasian L, Kotz H, Raggio M, Figg WD, Kohn EC. A phase I study of paclitaxel and continuous daily CAI in patients with refractory solid tumors. Cancer Biol Ther. 2009; 8:1800–05.
42. Bauer KS, Figg WD, Hamilton JM, Jones EC, Premkumar A, Steinberg SM, Dyer V, Linehan WM, Pluda JM, Reed E. A pharmacokinetically guided Phase II study of carboxyamido-triazole in androgen-independent prostate cancer. Clin Cancer Res. 1999; 5:2324–29.
43. Berlin J, Tutsch KD, Arzoomanian RZ, Alberti D, Binger K, Feierabend C, Dresen A, Marnocha R, Pluda J, Wilding G. Phase I and pharmacokinetic study of a micronized formulation of carboxyamidotriazole, a calcium signal transduction inhibitor: toxicity, bioavailability and the effect of food. Clin Cancer Res. 2002; 8:86–94.
44. Dutcher JP, Leon L, Manola J, Friedland DM, Roth B, Wilding G, and Eastern Cooperative Oncology Group. Phase II study of carboxyamidotriazole in patients with advanced renal cell carcinoma refractory to immunotherapy: E4896, an Eastern Cooperative Oncology Group Study. Cancer. 2005; 104:2392–99.
45. Hussain MM, Kotz H, Minasian L, Premkumar A, Sarosy G, Reed E, Zhai S, Steinberg SM, Raggio M, Oliver VK, Figg WD, Kohn EC. Phase II trial of carboxyamidotriazole in patients with relapsed epithelial ovarian cancer. J Clin Oncol. 2003; 21:4356–63.
46. Kohn EC, Reed E, Sarosy G, Christian M, Link CJ, Cole K, Figg WD, Davis PA, Jacob J, Goldspiel B, Liotta LA. Clinical investigation of a cytostatic calcium influx inhibitor in patients with refractory cancers. Cancer Res. 1996; 56:569–73.
47. Kohn EC, Reed E, Sarosy GA, Minasian L, Bauer KS, Bostick-Bruton F, Kulpa V, Fuse E, Tompkins A, Noone M, Goldspiel B, Pluda J, Figg WD, Liotta LA. A phase I trial of carboxyamido-triazole and paclitaxel for relapsed solid tumors: potential efficacy of the combination and demonstration of pharmacokinetic interaction. Clin Cancer Res. 2001; 7:1600–09.
48. Omuro A, Beal K, McNeill K, Young RJ, Thomas A, Lin X, Terziev R, Kaley TJ, DeAngelis LM, Daras M, Gavrilovic IT, Mellinghoff I, Diamond EL, et al. Multicenter Phase IB Trial of Carboxyamidotriazole Orotate and Temozolomide for Recurrent and Newly Diagnosed Glioblastoma and Other Anaplastic Gliomas. J Clin Oncol. 2018; 36:1702–09.
49. Thomas LW, Lam C, Edwards SW. Mcl-1; the molecular regulation of protein function. FEBS Lett. 2010; 584:2981–89.
50. Bird GS, DeHaven WI, Smyth JT, Putney JW Jr. Methods for studying store-operated calcium entry. Methods. 2008; 46:204–12.
51. Jardin I, Rosado JA. STIM and calcium channel complexes in cancer. Biochim Biophys Acta. 2016; 1863:1418–26.
52. Lytton J, Westlin M, Hanley MR. Thapsigargin inhibits the sarcoplasmic or endoplasmic reticulum Ca-ATPase family of calcium pumps. J Biol Chem. 1991; 266:17067–71.
53. Breuleux M, Klopfenstein M, Stephan C, Doughty CA, Barys L, Maira SM, Kwiatkowski D, Lane HA. Increased AKT S473 phosphorylation after mTORC1 inhibition is rictor dependent and does not predict tumor cell response to PI3K/mTOR inhibition. Mol Cancer Ther. 2009; 8:742–53.
54. Laplante M, Sabatini DM. mTOR signaling in growth control and disease. Cell. 2012; 149:274–93.
55. Jing Z, Sui X, Yao J, Xie J, Jiang L, Zhou Y, Pan H, Han W. SKF-96365 activates cytoprotective autophagy to delay apoptosis in colorectal cancer cells through inhibition of the calcium/CaMKIIγ/AKT-mediated pathway. Cancer Lett. 2016; 372:226–38.
56. Wang YY, Zhao R, Zhe H. The emerging role of CaMKII in cancer. Oncotarget. 2015; 6:11725-11734. https://doi.org/10.18632/oncotarget.3955.
57. Mihaylova MM, Shaw RJ. The AMPK signalling pathway coordinates cell growth, autophagy and metabolism. Nat Cell Biol. 2011; 13:1016–23.
58. Ishikawa J, Ohga K, Yoshino T, Takezawa R, Ichikawa A, Kubota H, Yamada T. A pyrazole derivative, YM-58483, potently inhibits store-operated sustained Ca2+ influx and IL-2 production in T lymphocytes. J Immunol. 2003; 170:4441–49.
59. Chen S, Dai Y, Harada H, Dent P, Grant S. Mcl-1 down-regulation potentiates ABT-737 lethality by cooperatively inducing Bak activation and Bax translocation. Cancer Res. 2007; 67:782–91.
60. Lucas KM, Mohana-Kumaran N, Lau D, Zhang XD, Hersey P, Huang DC, Weninger W, Haass NK, Allen JD. Modulation of NOXA and MCL-1 as a strategy for sensitizing melanoma cells to the BH3-mimetic ABT-737. Clin Cancer Res. 2012; 18:783–95.
61. Alessandro R, Fontana S, Giordano M, Corrado C, Colomba P, Flugy AM, Santoro A, Kohn EC, De Leo G. Effects of carboxyamidotriazole on *in vitro* models of imatinib-resistant chronic myeloid leukemia. J Cell Physiol. 2008; 215:111–21.
62. Lambert PA, Somers KD, Kohn EC, Perry RR. Antiproliferative and antiinvasive effects of carboxyamido-triazole on breast cancer cell lines. Surgery. 1997; 122:372–78.
63. Chen C, Ju R, Shi J, Chen W, Sun F, Zhu L, Li J, Zhang D, Ye C, Guo L. Carboxyamidotriazole Synergizes with Sorafenib to Combat Non-Small Cell Lung Cancer through Inhibition of NANOG and Aggravation of Apoptosis. J Pharmacol Exp Ther. 2017; 362:219–29.
64. Guo L, Li ZS, Wang HL, Ye CY, Zhang DC. Carboxyamido-triazole inhibits proliferation of human breast cancer cells

via G(2)/M cell cycle arrest and apoptosis. Eur J Pharmacol. 2006; 538:15–22.

65. Yang JL, Qu XJ, Yu Y, Kohn EC, Friedlander ML. Selective sensitivity to carboxyamidotriazole by human tumor cell lines with DNA mismatch repair deficiency. Int J Cancer. 2008; 123:258–63.

66. Ge S, Rempel SA, Divine G, Mikkelsen T. Carboxyamido-triazole induces apoptosis in bovine aortic endothelial and human glioma cells. Clin Cancer Res. 2000; 6:1248–54.

67. Rodland KD, Wersto RP, Hobson S, Kohn EC. Thapsigargin-induced gene expression in nonexcitable cells is dependent on calcium influx. Mol Endocrinol. 1997; 11:281–91.

68. Gocher AM, Azabdaftari G, Euscher LM, Dai S, Karacosta LG, Franke TF, Edelman AM. Akt activation by Ca2+/calmodulin-dependent protein kinase kinase 2 (CaMKK2) in ovarian cancer cells. J Biol Chem. 2017; 292:14188–204.

69. Høyer-Hansen M, Jäättelä M. AMP-activated protein kinase: a universal regulator of autophagy? Autophagy. 2007; 3:381–83.

70. Yang J, Yu J, Li D, Yu S, Ke J, Wang L, Wang Y, Qiu Y, Gao X, Zhang J, Huang L. Store-operated calcium entry-activated autophagy protects EPC proliferation via the CAMKK2-MTOR pathway in ox-LDL exposure. Autophagy. 2017; 13:82–98.

71. Kim KD, Srikanth S, Yee MK, Mock DC, Lawson GW, Gwack Y. ORAI1 deficiency impairs activated T cell death and enhances T cell survival. J Immunol. 2011; 187:3620–30.

72. Hewavitharana T, Deng X, Wang Y, Ritchie MF, Girish GV, Soboloff J, Gill DL. Location and function of STIM1 in the activation of Ca2+ entry signals. J Biol Chem. 2008; 283:26252–62.

73. Yang N, Tang Y, Wang F, Zhang H, Xu D, Shen Y, Sun S, Yang G. Blockade of store-operated Ca(2+) entry inhibits hepatocarcinoma cell migration and invasion by regulating focal adhesion turnover. Cancer Lett. 2013; 330:163–69.

74. Tang BD, Xia X, Lv XF, Yu BX, Yuan JN, Mai XY, Shang JY, Zhou JG, Liang SJ, Pang RP. Inhibition of Orai1-mediated Ca^{2+} entry enhances chemosensitivity of HepG2 hepatocarcinoma cells to 5-fluorouracil. J Cell Mol Med. 2017; 21:904–15.

75. Motiani RK, Hyzinski-García MC, Zhang X, Henkel MM, Abdullaev IF, Kuo YH, Matrougui K, Mongin AA, Trebak M. STIM1 and Orai1 mediate CRAC channel activity and are essential for human glioblastoma invasion. Pflugers Arch. 2013; 465:1249–60.

76. Yang S, Zhang JJ, Huang XY. Orai1 and STIM1 are critical for breast tumor cell migration and metastasis. Cancer Cell. 2009; 15:124–34.

77. Chen YF, Chiu WT, Chen YT, Lin PY, Huang HJ, Chou CY, Chang HC, Tang MJ, Shen MR. Calcium store sensor stromal-interaction molecule 1-dependent signaling plays an important role in cervical cancer growth, migration, and angiogenesis. Proc Natl Acad Sci USA. 2011; 108:15225–30.

78. Schmidt S, Liu G, Liu G, Yang W, Honisch S, Pantelakos S, Stournaras C, Hönig A, Lang F. Enhanced Orai1 and STIM1 expression as well as store operated Ca2+ entry in therapy resistant ovary carcinoma cells. Oncotarget. 2014; 5:4799–810. https://doi.org/10.18632/oncotarget.2035.

79. Winters ME, Mehta AI, Petricoin EF 3rd, Kohn EC, Liotta LA. Supra-additive growth inhibition by a celecoxib analogue and carboxyamido-triazole is primarily mediated through apoptosis. Cancer Res. 2005; 65:3853–60.

80. Ju R, Guo L, Li J, Zhu L, Yu X, Chen C, Chen W, Ye C, Zhang D. Carboxyamidotriazole inhibits oxidative phosphorylation in cancer cells and exerts synergistic anti-cancer effect with glycolysis inhibition. Cancer Lett. 2016; 370:232–41.

81. Lesept F, Chevilley A, Jezequel J, Ladépêche L, Macrez R, Aimable M, Lenoir S, Bertrand T, Rubrecht L, Galea P, Lebouvier L, Petersen KU, Hommet Y, et al. Tissue-type plasminogen activator controls neuronal death by raising surface dynamics of extrasynaptic NMDA receptors. Cell Death Dis. 2016; 7:e2466.